Liquid Crystals
Publication details, including instructions for authors and subscription information:
http://www.informaworld.com/smpp/title~content=t713926090

Twist-grain-boundary transitions in a chiral tolane compound

G. S. Iannacchione

Online publication date: 06 August 2010

To cite this Article Iannacchione, G. S.(1999) 'Twist-grain-boundary transitions in a chiral tolane compound', Liquid Crystals, 26: 1, 69 — 74
To link to this Article: DOI: 10.1080/026782999205560
URL: http://dx.doi.org/10.1080/026782999205560

LIQUID CRYSTALS, 1999, VOL. 26, NO. 1, 69–74

Twist-grain-boundary transitions in a chiral tolane compound

G. S. IANNACCHIONE and C. W. GARLAND*

Department of Chemistry and Center for Material Science and Engineering, Massachusetts Institute of Technology, Cambridge, Massachusetts 02139, USA

(*Received 3 July 1998; accepted 10 August 1998*)

High resolution calorimetric studies have been carried out on the chiral compound methylheptyloxydifluorooctyloxybenzoyloxytolane (8BTF$_2$O$_1$M$_7$). The tilt tendency is greater in this compound than in several other structurally similar fluorinated tolane liquid crystals, and it exhibits tilted chiral smectic C (SmC*) and tilted twist-grain-boundary (TGB$_C$) phases but not the untilted SmA or TGB$_A$ phases. The data confirm the presence of two tilted TGB$_C$ phases denoted TGB$_1$ and TGB$_2$. The TGB$_1$–TGB$_2$ first-order transition exhibits considerable hysteresis and a very small latent heat. There is no rounded excess heat capacity peak in the cholesteric N* phase associated with the non-transitional evolution of a chiral line liquid N_L^*, although such a feature has been observed in other fluorinated tolanes with a smaller tilt tendency.

1. Introduction

During the past ten years, there have been numerous studies of chiral liquid crystals that exhibit twist-grain-boundary phases with a regular stack of periodic grain boundaries separating regions of smectic A order (TGB$_A$) or tilted smectic C order (TGB$_C$). These phases were predicted theoretically by Renn and Lubensky [1, 2], and the TGB$_A$ phase was first observed experimentally by Goodby and coworkers [3–5]. Of special interest are investigations of several homologous series of fluorinated compounds with a tolane core and having the general formula

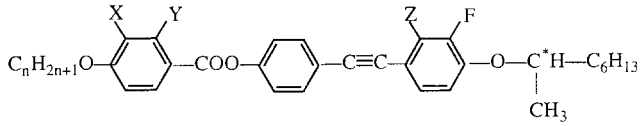

The series denoted as *n*FBTFO$_1$M$_7$, where $X = F$ and $Y = Z = H$, is 3-fluoro-4[(*R*) or (*S*)-1-methylheptyloxy]-4′-(4-alkoxy-3-fluorobenzoyloxy)tolane. These compounds display primarily a TGB$_A$ phase [6] with a very narrow TGB$_C$ range for $n \geqslant 12$ [7]. This TGB$_A$ phase and associated transitions have been well characterized structurally [6] and calorimetrically [8]. The homologous series *n*F$_2$BTFO$_1$M$_7$, where $X = Y = F$ and $Z = H$, is the 2,3-difluorobenzoyloxy analogue of *n*FBTFO$_1$M$_7$. These compounds exhibit both the TGB$_A$ phase ($n < 11$) and the TGB$_C$ phase ($n > 10.5$); the TGB structures and transitions have been extensively studied [9–12]. The series *n*BTF$_2$O$_1$M$_7$, where $X = Y = H$ and $Z = F$, exhibits TGB$_C$ and SmC* phases but no TGB$_A$ or SmA phases and monotropic ferri- as well as antiferro-electric smectic C* phases have also been observed just above room temperature [13, 14]. Thus the tilting tendency for a given alkoxy chain length increases as one goes from *n*FBTFO$_1$M$_7$ to *n*F$_2$BTFO$_1$M$_7$ to *n*BTF$_2$O$_1$M$_7$.

High-resolution calorimetric studies of *n*FBTFO$_1$M$_7$ and *n*F$_2$BTFO$_1$M$_7$ compounds [8, 12] have revealed two interesting features that are not yet fully understood. First, there is a large rounded excess heat capacity peak in the cholesteric region that has no associated latent heat. This has been ascribed in [8] and [12] as due to a nontransitional evolution from the normal twisted nematic N* to a chiral line liquid denoted as N_L^*. Such a N_L^* structure has been predicted by Kamien and Lubensky [15] and corresponds to a *liquid* of screw dislocations with significant *short-range* TGB structure. N* and N_L^* have the same global symmetry and are not thermodynamically distinct phases. These regions are analogues of the normal metal in an external field and the Abrikosov vortex liquid in high-T_c superconductors, whereas TGB phases are analogue of the Abrikosov vortex lattice. Second, there is thermal evidence in 11F$_2$BTFO$_1$M$_7$ and 12F$_2$BTFO$_1$M$_7$ [12] of two closely spaced first-order transitions where a single TGB$_C$–N* transition was expected on the basis of initial structural work [9, 10]. In [12] this phase sequence was denoted as TGB_C^{α}–TGB_C^{β}–N_L^*. However, there is no structural information about the TGB_C^{β} phase since it has a very narrow stability range ($\leqslant 0.07$ K).

The most extensively studied of the *n*BTF$_2$O$_1$M$_7$ series is 8BTF$_2$O$_1$M$_7$ [14]. DSC heating scans indicated that there were two TGB$_C$ phases, denoted TGB$_1$ and TGB$_2$ [14], and the phase sequence SmC*–TGB$_1$–TGB$_2$–N*

*Author for correspondence.

was reported. The present investigation involves a high resolution calorimetric study of $8BTF_2O_1M_7$. This system is of interest since the tilting tendency is significantly larger than in the related compounds $nFBTFO_1M_7$ and $nF_2BTFO_1M_7$, i.e. there are no TGB_A or SmA phases. Furthermore, both the N* range and the TGB_C range (especially that of TGB_2) are much wider than those of analogous phases in $11F_2BTFO_1M_7$ and $12F_2BTFO_1M_7$. Our calorimetric data show no indications of a rounded N^*–N_L^* excess heat capacity feature, which agrees well with the previously reported trend of decreasing N^*–N_L^* enthalpy as the tilt tendency increases [12]. The presence of a first-order TGB_1–TGB_2 transition has been confirmed on both heating and cooling scans.

2. Experimental results

The compound $8BTF_2O_1M_7$, 4[(*S*)-1-methylheptyloxy]-2,3-difluoro-4′-(4-octyloxybenzoyloxy)tolane, with a molecular weight of $590.7\ g\ mol^{-1}$, was synthesized at the Centre de Recherche Paul Pascal following the procedure described in [14]. The *S* enantiomer investigated here is the same enantiomer that was studied in [14]. The reported phase sequence [13, 14] on the basis of DSC scans is

$$\underset{\sim 312.8}{SmC_A^*} \leftarrow \underset{\sim 313.8}{SmC_{FI}^*} \leftarrow \underset{335.5}{K} \rightarrow \underset{359.35}{SmC^*} \underset{360.65}{TGB_1} \underset{361.05}{TGB_2} \underset{\sim 398.2}{N^*} \underset{\sim 398.7}{BP} I$$

where the transition temperatures in Kelvin are values obtained on heating (except for the monotropic transitions which were obtained on cooling scans). Preliminary DSC heating scans at $+0.5$ and $+1\ K\ min^{-1}$ were carried out on the $8BTF_2O_1M_7$ sample used in the present study, the transition temperatures agreeing well (within ± 0.4 K) with those cited above. On the basis of a comparison of DSC transition temperatures with those obtained with high-resolution ac calorimetry, it appears that there is a calibration error in the DSC thermometry. We estimate that the DSC temperatures are ~ 0.75 K lower than the true values. This systematic DSC calibration error is comparable to the value of ~ 1 K observed for $nFBTFO_1M_7$ [16].

The present study covered the 330–400 K temperature range, but detailed measurements were focused on the SmC*–TGB_1–TGB_2–N* region. This notation used in [14] for the TGB_C phases of $8BTF_2O_1M_7$ will be retained. Although it is quite possible that there is an isomorphism between these TGB_1/TGB_2 phases and the $TGB_C^{\alpha}/TGB_C^{\beta}$ phases of $nBTFO_1M_7$ [12], it seems better to use different notations to allow for the possibility that different structures are involved.

A small mass (26 mg) of $8BTF_2O_1M_7$ was degassed under vacuum and then cold-weld sealed into a thin silver cell. Thermal measurements were carried out in a computerized calorimeter capable of automated operation in either an ac mode or a ramped relaxation mode called non-adiabatic scanning (nas). This calorimeter and the appropriate equations for analyzing the observed T_{ac} response to the $P_o\exp(i\omega t)$ ac heat input or the observed dT/dt response to a linearly ramped dc heater power input are described elsewhere [17]. The essential difference between the two modes of operation is that the ac mode measures heat capacity C_p directly and is capable of very slow scan rates. However, it can at best provide only qualitative information about the presence of a two-phase coexistence region at a first-order transition. The nas mode measures the enthalpy H as a function of temperature and thus yields both C_p values in one-phase regions and latent heats at first-order transitions. The procedure for a nas run was as follows. The bath temperature was stabilized ~ 1.5 h at an initial value and held constant at this value during a pair of scans; the dc heater power to the sample was first ramped down to zero over 500 s (resulting in a cooling of ~ 0.96 K); after a ~ 500 s waiting period for sample temperature equilibration, the heater power was ramped up over 500 s (resulting in a heating of ~ 0.96 K). Following this sequence, the bath temperature was set at a new lower value and stabilized there for ~ 1.5 h prior to carrying out another pair of scans.

On the initial ac heating scan, a sharp melting transition was observed at 336.04 K, in good agreement with the value reported by Navailles *et al.* [13, 14]. An overview of C_p(ac) data obtained on a later scan for the range 350–400 K is shown in figure 1. These data were obtained at an a.c. frequency $\omega = 2\omega_o$, where $\omega_o = 2\pi f_o = 0.196\ s^{-1}$ (or $f_o = 31.25$ mHz) is the standard operating frequency previously used with this calorimeter. The data in figure 1 were obtained on heating at a scan rate of $+0.2\ K\ h^{-1} = +3.3\ mK\ min^{-1}$. The transitions that are obvious from figure 1 are TGB_2–N* at 360.45 K and BP–I at 396.0 K. Both these transitions undergo a downward drift in the transition temperature dependent on the length of time that the sample is held at high temperatures. The drift rate is quite rapid (about $-0.2\ K\ day^{-1}$) during the first few days and then becomes much slower ($-3\ mK\ day^{-1}$) for longer periods. Analogous drifts in transition temperatures were also observed for $nF_2BTFO_1M_7$ compounds [12]. Since the data in figure 1 were obtained on run 5 after 30 days at temperatures above 350 K, we estimate the transition temperatures extrapolated back to $t = 0$ are 361.85 K for TGB_2–N* and 399.3 K for BP–I. These 'zero-time' transition temperatures agree well with the corrected DSC values from [14] and those obtained at MIT. A confirmation of these zero-time extrapolated values is the fact that the TGB_2–N* transition was observed at

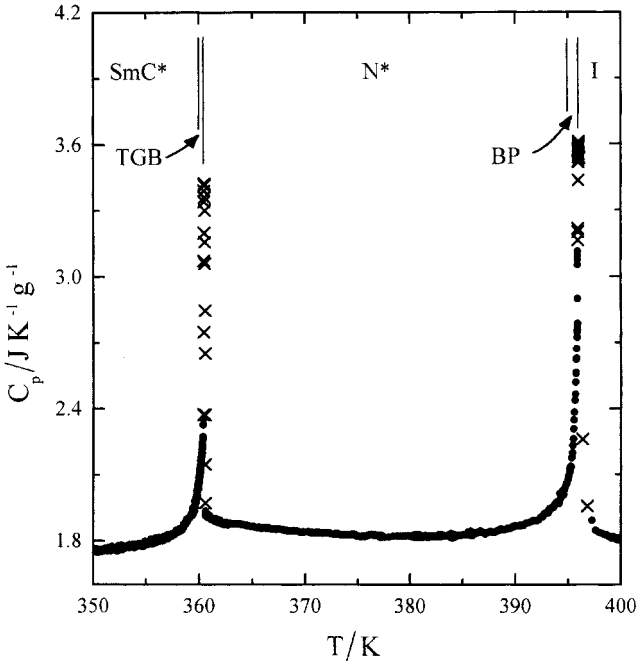

Figure 1. C_p(ac) data for 8BTF$_2$O$_1$M$_7$(S). These data were obtained on a heating run at frequency $2\omega_o$ and a scan rate of $+0.2$ K h^{-1}. Points denoted by crosses are anomalous C_p values obtained in a two-phase coexistence region.

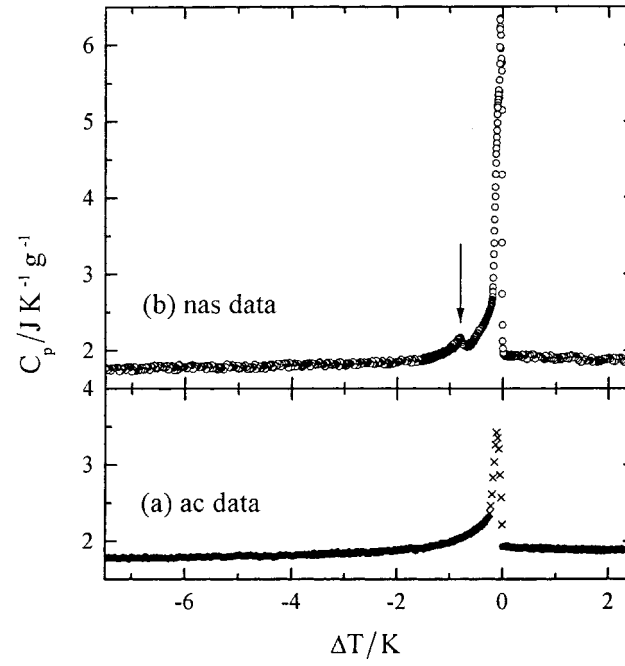

Figure 2. 8BTF$_2$O$_1$M$_7$ (S) heat capacity obtained on cooling from the N* to SmC* phase; $\Delta T = T - T$(TGB$_2$–N*). (*a*) C_p(ac) data at $\omega_o/2$ ($f = 15.6$ mHz); as in figure 1, the crosses indicate data points in the N* + TGB$_2$ two-phase coexistence region. (*b*) C_p(nas) data; the arrow indicates the TGB$_1$–TGB$_2$ transition on cooling.

361.85 K on the first heating run, where any drift is negligible due to the short time the sample had been at high temperatures.

Anomalies in the phase shift between $T_{ac}(\omega)$ and $P_{ac}(\omega)$ indicate two-phase coexistence at a first-order transition and interphase conversion during the T_{ac} oscillation [17]. Such anomalies were observed at both the TGB$_2$–N* and the BP–I transition. Heat capacity points in figure 1 that are frequency-dependent apparent values obtained in a two-phase coexistence region are denoted by the symbol ×. All other C_p(ac) data points are frequency independent (as judged by comparing data obtained at $2\omega_o$ and $\omega_o/2$) and exhibit no phase shift anomalies.

The most important aspect of the data in figure 1 is the absence of any broad rounded excess C_p peak in the middle of the N* phase. This disappearance of a N*–N$_L^*$ feature will be discussed in §3.1. A more detailed study of the N*–BP–I region reveals a small excess C_p(N*–BP) peak ~0.35 K below the large BP–I peak, but the behaviour in this region will not be discussed further.

Figure 2 provides a more detailed view of calorimetric data in the SmC*–TGB–N* region. Shown in figure 2 (*a*) are C_p(ac) data obtained on a cooling run at frequency $\omega_o/2$ and a scan rate of -0.135 K h^{-1}. Figure 2 (*b*) shows non-adiabatic scan (nas) data obtained from cooling ramps with $dT/dt \approx -6.9$ K h^{-1} $= -0.115$ K min^{-1}. Note that these ramp rates are much slower than DSC scan rates (0.5–1.0 K min^{-1}) but much faster than ac scan rates. Comparison of figures 2 (*a*) and 2 (*b*) shows that both ac and nas data clearly show the prominent TGB$_2$–N* first-order transition with C_p(nas) ≥ C_p(ac) in the two-phase coexistence region. Also there is a small excess C_p(nas) peak at the TGB$_1$–TGB$_2$ transition which is not observed in the C_p(ac) data. Both these features are analogous to those observed in a high-resolution study of N*–BP$_I$–BP$_{III}$–I transitions in a highly chiral liquid crystal without TGB phases [18]. C_p(ac) data as a function of $\Delta T = T - T$(TGB–N*) was the same on heating and cooling runs, but the C_p(nas) data differed on heating and cooling in the TGB$_1$–TGB$_2$ region.

Figure 3 shows the hysteresis in the TGB$_1$–TGB$_2$ transition observed in the nonadiabatic scanning data. On cooling, the width of the TGB$_2$ phase, T(TGB$_2$–N*) − T(TGB$_1$–TGB$_2$), is 0.74 K and on heating it is 0.33 K (which is in good agreement with the value 0.4 K from DSC heating scans [14]). Taking the midpoint of these heating and cooling transition temperatures, we estimate the 'zero-time' equilibrium transition temperature to be 361.32 K. Also shown in figure 3 is a solid line representing the C_p(ac) variation given in figure 2 and an arrow indicating the expected position

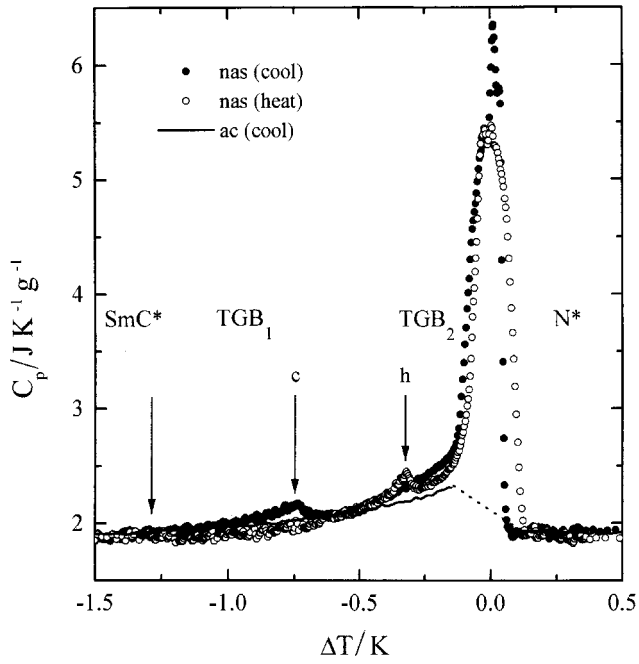

Figure 3. Detailed view of non-adiabatic scanning (nas) data obtained on heating and cooling scans; $\Delta T = T - T(\mathrm{TGB_2}\text{–N*})$. The solid line represents the one-phase C_p(ac) variation, and the dashed line approximates the non-transitional effective C_p(ac) behaviour in the two-phase N* + $\mathrm{TGB_2}$ coexistence region.

of the SmC*–$\mathrm{TGB_1}$ transition based on DSC heating scans carried out at MIT. Discussion of the thermal behaviour in the $\mathrm{TGB_1}$–$\mathrm{TGB_2}$ transition region and the absence of an excess heat capacity peak at the SmC*–$\mathrm{TGB_1}$ transition will be given in §3.

Integration of the non-adiabatic scanning data as described in [8, 12, 18] yields a $\mathrm{TGB_2}$–N* latent heat L of 0.53 J g^{-1} and one might also include the pretransitional enthalpy $\delta H = \int [C_p(\mathrm{ac}) - C_p(\mathrm{background})]\,dT = 1.16$ J g^{-1} associated with the C_p(ac) 'wing' over a 25 K range above and below the $\mathrm{TGB_2}$–N* transition. This total transitional enthalpy of ~1.7 J g^{-1} can be compared with less accurate DSC values of 1.2 J g^{-1} (MIT, +1 K min^{-1} scan) or 0.485 J g^{-1} ([14], +0.5 K min^{-1} scan).

3. Discussion

3.1. *Absence of N*–N_L^* heat capacity peak*

In contrast to the behaviour of $n\mathrm{FBTFO_1M_7}$ and $n\mathrm{F_2BTFO_1M_7}$ compounds, there is no indication of a broad and rounded N*–$\mathrm{N_L^*}$ C_p peak in $8\mathrm{BTF_2O_1M_7}$. In the former compounds, the integrated enthalpy δH of this feature is substantial, ranging from 1.8 J g^{-1} in $9\mathrm{FBTFO_1M_7}$ to 0.8 J g^{-1} in $11\mathrm{FBTFO_1M_7}$ and 1.4 J g^{-1} in $10\mathrm{F_2BTFO_1M_7}$ to 0.28 J g^{-1} in $12\mathrm{F_2BTFO_1M_7}$ [8, 12]. This marked decrease in δH as the tilting tendency increases, and the complete absence of any analogous feature in $8\mathrm{BTF_2O_1M_7}$, strongly suggests that any twist-grain-boundary ordering in the '$\mathrm{N_L^*}$ phase' of $n\mathrm{FBTFO_1M_7}$ and $\mathrm{F_2BTFO_1M_7}$ is due to $\mathrm{TGB_A}$-like structures.

The nature of the '$\mathrm{N_L^*}$ phase' is not yet resolved. In [8] and [12], it was proposed that there is a non-transitional evolution of short-range TGB order on cooling as N* converts into a chiral line liquid denoted as $\mathrm{N_L^*}$. This N*–$\mathrm{N_L^*}$ assignment is consistent with the thermal evidence for $n\mathrm{FBTFO_1M_7}$ and $n\mathrm{F_2BTFO_1M_7}$: no latent heat, and very broad (5–10 K) and very rounded excess heat capacity peaks that are nonsingular [8, 12]. However, a recent X-ray study of $10\mathrm{F_2BTFO_1M_7}$ [11] indicates that this purported $\mathrm{N_L^*}$ region may possibly be an incommensurate $\mathrm{TGB_A}$ phase, followed at lower temperatures in that compound by a commensurate $\mathrm{TGB_A}$ phase. Thus the sequence $\mathrm{TGB_A}$(com)–$\mathrm{TGB_A}$(inc)–N* with two thermodynamic transitions may occur in $10\mathrm{F_2BTFO_1M_7}$ instead of $\mathrm{TGB_A}$–$\mathrm{N_L^*}$–N*.

The critical issue is whether or not the $\mathrm{TGB_A}$ order is long range or short range in such a '$\mathrm{N_L^*}$' region. If a chiral line liquid $\mathrm{N_L^*}$ does exist in $10\mathrm{F_2BTO_1M_7}$, the short-range $\mathrm{TGB_A}$ order must be well developed since the excess N*–$\mathrm{N_L^*}$ enthalpy δH is large. Thus the issue becomes how well X-ray data can distinguish between highly developed short range order and long range order in a $\mathrm{TGB_A}$(inc) phase with finite smectic slab thicknesses. It is important to check the smectic order along the pitch direction as well as in the plane perpendicular to the helical axis studied in [11]. If $10\mathrm{F_2BTFO_1M_7}$ does exhibit a true transition from N* to $\mathrm{TGB_A}$(inc), why is the associated excess heat capacity non-singular? It should be noted that the observed broad $C_p(T)$ variation is unlike that characteristic of typical finite-size truncation effects.

The interesting issue for $8\mathrm{BTF_2O_1M_7}$ is not only the absence of a N*–$\mathrm{N_L^*}$ rounded C_p feature like that discussed above but also the clear presence of a conventional pretransitional excess heat capacity in the N* phase at temperatures above the $\mathrm{TGB_2}$–N* transition. As shown in figure 1, this excess C_p extends over ~20 K and the integrated enthalpy $\delta H'$ associated with this high temperature C_p wing is ~0.5 J g^{-1}, which is comparable to δH(N*–$\mathrm{N_L^*}$) for $11\mathrm{FBTFO_1M_7}$ and $11\mathrm{F_2BTFO_1M_7}$. X-ray data in a 3 K range above $T(\mathrm{TGB_2}\text{–N*})$ reveal diffuse scattering that corresponds to truly short range $\mathrm{TGB_C}$-like ordering in the N* phase of $8\mathrm{BTF_2O_1M_7}$ [14].

3.2. *Two TGB_C phases*

Figure 3 confirms the existence of a $\mathrm{TGB_1}$–$\mathrm{TGB_2}$ transition between two $\mathrm{TGB_C}$ phases as suggested by earlier data [14]. The high temperature $\mathrm{TGB_2}$ phase

in $8BTF_2O_1M_7$ is ~ 0.5 K wide, but the first-order TGB_1–TGB_2 transition is kinetically sluggish and there is a large hysteresis. An analogous pair of TGB_C phases, denoted TGB_C^{α} and TGB_C^{β}, has been reported in $11F_2BTFO_1M_7$ and $12F_2BTFO_1M_7$ although these TGB_C phases have only a narrow range of stability (~ 0.73 K for TGB_C^{α} and ~ 0.06 K for TGB_C^{β}) [12]. These $TGB_C^{\alpha}/TGB_C^{\beta}$ and TGB_1/TGB_2 pairs may well be structurally related but there are several differences in the thermal behaviour of $8BTF_2O_1M_7$ and $nF_2BTFO_1M_7$. In contrast to the behaviour of $8BTF_2O_1M_7$, TGB_C^{α}–TGB_C^{β} transitions were clearly observed in ac calorimetry as low temperature shoulders on the TGB_C^{β}–N_L^* heat capacity peak and as distinct ac phase shift anomalies, and, furthermore, no hysteresis was observed. Both these differences may be due to substantial differences in the rates of TGB_C^{α}–TGB_C^{β} and TGB_1–TGB_2 phase conversion. However, there are also considerable differences in the transition enthalpies. For $nF_2BTFO_1M_7$, the latent heats for TGB_C^{β}–N_L^* and TGB_C^{α}–TGB_C^{β} transitions were $0.125 + 0.02 = 0.145$ J g^{-1} for $n = 11$ and $0.255 + 0.04 = 0.295$ J g^{-1} for $n = 12$ [12]. For $8BTF_2O_1M_7$, $L(TGB_2$–$N^*) = 0.53$ J g^{-1} and $L(TGB_1$–$TGB_2)$ is estimated to be ~ 0.02 J g^{-1}. The latter value is very difficult to determine in view of the hysteresis and a sluggish conversion which suggests that some of the transition enthalpy is smeared out over almost 1 K.

A recent extension has been made of the mean field Chen–Lubensky theoretical approach used originally in [1, 2] to analyse the phase behaviour of chiral molecules. This new theoretical work of Luk'yanchuk [19] considers the stability of four structurally different TGB_C phases. The TGB_{Cp} and TGB_{Ct} phases have SmC slabs (no director precession) where the tilted smectic layers are parallel to or tilted with respect to the pitch axis, respectively. The TGB_{C*} phase has SmC* slabs, and a novel TGB_{2q} phase is also predicted. The latter phase, which corresponds to a superposition of two degenerate TGB_{Ct} phases with opposite layer inclinations to the pitch axis, is predicted to lie in a narrow temperature range between the N* and TGB_{Ct} phases.

The original Renn–Lubensky theory [1, 2] resulted in the prediction of TGB_{Cp} and TGB_{C*} phases. X-ray experiments [10] and theoretical estimates by Dozov [20] show that the TGB_{Ct} phase is more stable than the TGB_{Cp} phase. At present, the existence of the TGB_{C*} phase is uncertain since there is no clear experimental evidence for such a phase. Thus we will focus further discussion on the TGB_{Ct} and TGB_{2q} phases.

X-ray studies have shown that the TGB_C^{α} phase of $12F_2BTFO_1M_7$ [10] and the TGB_1 phase of $8BTF_2O_1M_7$ [14] are both commensurate TGB_{Ct} phases with 16–20 blocks per pitch for the former and 11 blocks for the latter. It is tempting to suggest that the TGB_C^{β} phase and the TGB_2 phase might have the same structure. They might be TGB_{2q} phases as predicted in [19] or perhaps TGB_C phases with 'curved' smectic layers (i.e., TGB_A-like near the grain boundaries and TGB_{Ct}-like in the center of a slab) as proposed by Dozov [21]. The experimental situation concerning these structures is very incomplete. Due to the very narrow TGB_C^{β} range in $nF_2BTFO_1M_7$, no X-ray data have yet been taken in this phase. The few χ scans taken in the TGB_2 phase of $8BTF_2O_1M_7$ showed no azimuthal modulation [14], which might indicate that this is a TGB_{Ct}(inc) phase. However, these data were taken with only medium resolution and artifacts such as a large angular mosaic or a large number of blocks per pitch that would smear the scattered intensity cannot be ruled out. A high resolution X-ray study of (1) detailed χ scans in the TGB_2 phase and also (2) diffuse scattering due to short range TGB order above the TGB_2–N* transition, associated with the excess heat capacity discussed in §3.1, would be of great value.

3.3. *SmC*–TGB$_C$ transition*

The SmC*–TGB_C^{α} transition in $nF_2BTFO_1M_7$ was very difficult to observe in C_p(ac) data but it was revealed by a step discontinuity in the ac phase shift, which showed a hysteresis of 0.85 K for $n = 11$ and 0.50 K for $n = 12$ [12]. Furthermore, the latent heat, $L = 0.05$ J g^{-1} for $n = 11$ and $L = 0.125$ J g^{-1} for $n = 12$, was easily determined from nas scans. Thus this SmC*–TGB_C^{α} transition is a sluggish first-order transition where coexisting SmC* and TGB_C^{α} phases cannot interconvert rapidly enough to follow T_{ac} oscillations at frequency ω_o.

In contrast to $nF_2BTFO_1M_7$, no calorimetric evidence of the analogous SmC*–TGB_1 transition in $8BTF_2O_1M_7$ was observed in either ac or nas scans. The only thermal evidence for this transition is from DSC heating scans. DSC scans yielded transition enthalpies of ~ 0.045 J g^{-1} ([14], $+0.5$ K min^{-1}) to ~ 0.08 J g^{-1} (MIT, $+1$ K min^{-1}).

A possible explanation of these observations is that the development of structural ordering in the TGB_1 phase is slow and, furthermore, the heat capacities of fully equilibrated SmC* and TGB_1 phases are essentially identical and the equilibrium latent heat is very small for this transition. If this were so, slow ac and nas scans would show no thermal evidence of this transition while rapid DSC heating scans would involve a transition from SmC* to a non-equilibrium TGB_1 state with higher disorder (and thus higher enthalpy) than the equilibrium TGB_1. In any event, optical pitch data and X-ray data both unambiguously indicate the presence of the SmC*–TGB_1 transition at ~ 360.5 K [14].

The authors wish to thank L. Navailles for numerous helpful discussions and H. T. Nguyen for providing the

8BTF2OlM7 sample. This work was supported by the MRSEC program of the National Science Foundation under Grant No. DMR 94-00334.

References

[1] Renn, S. R., and Lubensky, T. C., 1988, *Phys. Rev. A*, **38,** 2132; Renn, S. R., and Lubensky, T. C., 1991, *Mol. Cryst. liq. Cryst.*, **209,** 349.

[2] Renn, S. R., 1992, *Phys. Rev. A*, **45,** 953.

[3] Goodby, J. W., Waugh, M. A., Chin, E., Pindak, R., and Patel, J. S., 1989, *J. Am. chem. Soc.*, **111,** 8119.

[4] Strajer, G., Pindak, R., Waugh, M. A., and Goodby, J. W., 1990, *Phys. Rev. Lett.*, **64,** 1545.

[5] Goodby, J. W., Nishigama, I., Slaney, A. J., Booth, C. J., and Toyne, K. J., 1993, *Liq. Cryst.*, **14,** 37 and references therein.

[6] Bouchta, A., Nguyen, H. T., Achard, M. F., Hardouin, F., Destrade, C., Twieg, R. J., Maaroufi, A., and Isaert, N., 1992, *Liq. Cryst.*, **12,** 575.

[7] Bouchta, A., Nguyen, H. T., Navailles, L., Barois, P., Destrade, C., Bougrioua, F., and Isaert, N., 1995, *J. mater. Chem.*, **5,** 2079.

[8] Chan, T., Garland, C. W., and Nguyen, H. T., 1995, *Phys. Rev. E*, **52,** 5000.

[9] Nguyen, H. T., Bouchta, A., Navailles, L., Barois, P., Isaert, N., Twieg, R. J., Maaroufi, A., and Destrade, C., 1992, *J. Phys. II Fr.*, **2,** 1889.

[10] Navailles, L., Barois, P., and Nguyen, H. T., 1993, *Phys. Rev. Lett.*, **71,** 545; Navailles, L., Pindak, R., Barois, P., and Nguyen, H. T., 1995, *Phys. Rev. Lett.*, **74,** 5224.

[11] Navailles, L., Pansu, B., Gorre-Talini, L., and Nguyen, H. T., *Phys. Rev. Lett.* (submitted).

[12] Navailles, L., Garland, C. W., and Nguyen, H. T., 1996, *J. Phys. II Fr.*, **6,** 1243.

[13] Navailles, L., 1994, PhD thesis, University of Bordeaux I (unpublished).

[14] Navailles, L., Nguyen, H. T., Barois, P., Isaert, N., and de Lord, P., 1996, *Liq. Cryst.*, **20,** 653. It should be noted that there is a typographical error in the melting point reported here. It should be 62.4°C, not 52.4°C.

[15] Kamien, R. D., and Lubensky, T. C., 1993, *J. Phys. I Fr.*, **3,** 2131.

[16] Chan, T., 1995, PhD. thesis, MIT (unpublished).

[17] Yao, H., Chan, T., and Garland, C. W., 1995, *Phys. Rev. E*, **51,** 4585.

[18] Kutnjak, Z., Garland, C. W., Schatz, C. G., Collings, P. J., Booth, C. J., and Goodby, J. W., 1996, *Phys. Rev. E*, **53,** 4955. See the $X = 0.40$ data in figures 4 and 5 of this paper.

[19] Luk'yanchuk, I., 1998, *Phys. Rev. E*, **57,** 574.

[20] Dozov, I., 1995, *Phys. Rev. Lett.*, **74,** 4245. In this paper, the TGB_{Ct} phase is called a twist-melted-grain boundary (TMGB) phase, which emphasizes the fact that the smectic order parameter should vanish at the grain boundaries.

[21] Dozov, I., private communication.